ORIGINAL ARTICLE

Impact of intraventricular haemodynamic forces misalignment on left ventricular remodelling after myocardial infarction

Domenico Filomena[1]* iD , Sara Cimino[1], Sara Monosilio[1], Nicola Galea[2,3], Giuseppe Mancuso[2], Marco Francone[2], Giovanni Tonti[4], Gianni Pedrizzetti[5], Viviana Maestrini[1], Francesco Fedele[1] and Luciano Agati[1]

[1]Department of Clinical, Internal, Anesthesiology and Cardiovascular Sciences, 'Sapienza' University of Rome, Policlinico Umberto I, Viale del Policlinico 155, Rome, 00161, Italy; [2]Department of Radiological, Oncological, and Pathological Sciences, 'Sapienza' University of Rome, Rome, Italy; [3]Department of Experimental Medicine, 'Sapienza' University of Rome, Rome, Italy; [4]Cardiology Division, 'G. D'Annunzio' University, Chieti, Italy; [5]Department of Engineering and Architecture, University of Trieste, Trieste, Italy

Abstract

Aims Altered left ventricular (LV) haemodynamic forces (HDFs) have been associated with positive and negative remodelling after pathogenic or therapeutic events. We aimed to identify LV HDFs patterns associated with adverse LV remodelling (aLVr) in reperfused segment elevation myocardial infarction (STEMI) patients.

Methods and results Forty-nine acute STEMI patients underwent cardiac magnetic resonance (CMR) at 1 week (baseline) and after 4 months (follow-up). LV HDFs were computed at baseline from cine CMR long axis data sets, using a novel technique based on endocardial boundary tracking, both in apex-base (A-B) and latero-septal (L-S) directions. HDFs distribution was evaluated by L-S over A-B HDFs ratio (L-S/A-B HDFs ratio %). HDFs parameters were computed over the entire heartbeat, in systole and diastole. At baseline, aLVr patients had lower systolic L-S HDF (2.7 ± 0.9 vs. 3.6 ± 1%; *P* = 0.027) and higher diastolic L-S/A-B HDF ratio (28 ± 14 vs. 19 ± 6%; *P* = 0.03). At univariate logistic regression analysis, higher infarct size [odds ratio (OR) 1.05; 95% confidence interval (CI) 1.01–1.1; *P* = 0.04], higher L-S/A-B HDFs ratio (OR 1.1; 95% CI 1.01–1.2; *P* = 0.05) and lower L-S HDFs (OR 0.41; 95% CI 0.2–0.9; *P* = 0.04) were associated with aLVr at follow-up. In the multivariable logistic regression analysis, diastolic L-S/A-B HDF ratio remained the only independent predictor of aLVr (OR 1.1; 95% CI 1.01–1.2; *P* = 0.04).

Conclusions Misalignment of diastolic haemodynamic forces after STEMI is associated with aLVr after 4 months.

Introduction

Cardiac remodelling following acute myocardial infarction (MI) has been widely described. The single best predictor of adverse left ventricular remodelling (aLVr) is infarct size (IS) determined by cardiac magnetic resonance (CMR) imaging.[1] Other known predictors of post-infarction aLVr are anterior localization of infarct,[1] the presence of microvascular obstruction (MVO)[2] and intra-myocardial haemorrhage (IMH).[3] Neurohormonal activation promotes left ventricular remodelling (LVr), and modulation of β-adrenergic and renin-angio-tensin pathways is the best known strategy for preventing post-infarct heart failure.[4] Recent developments in cardiac fluid-dynamics imaging have heightened the interest about haemodynamic forces (HDFs) patterns associated with cardiac adaptations.[5] However, their association with cardiac adaptation after MI has not been investigated. We sought to evaluate HDFs and their influence on post-infarction aLVr in a cohort of patients with reperfused segment elevation MI (STEMI) using a novel technique based on endocardial borders tracking of steady-state free-precession cineMR data sets.

Methods

Study population

Forty-nine acute STEMI patients underwent CMR at 1 week (baseline) and 4 months (follow-up) after MI. Inclusion criteria were (i) clinical diagnosis of STEMI according current guidelines (STEMI guidelines), (ii) successful treatment with percutaneous coronary intervention (PCI) within 12 h from symptoms onset and (iii) sinus rhythm. Exclusion criteria were prior MI or revascularization, cardiogenic shock, atrial fibrillation, plasma creatinine > 2 mg/dL and claustrophobia or other contraindications to CMR. Twenty-one non-athletic healthy individuals (HC) underwent CMR as a control group for HDFs assessment. The study was conducted in accordance with the Declaration of Helsinki. Local ethical review boards approved the study, and all patients gave written informed consent.

Cardiovascular magnetic resonance acquisition

Cardiac magnetic resonance studies were performed using a commercial 1.5 T unit (Avanto-Siemens, Erlangen, Germany). Breath-hold steady-state free-precession cineMR images were acquired in cardiac vertical and horizontal long axis and short axis with full coverage of the ventricles. Area at risk (AAR) was assessed using black-blood short tau inversion recovery T2-weighted sequence (T2w imaging) acquired in cardiac long and short axis. After contrast administration, breath-hold, two-dimensional inversion recovery, segmented gradient-echo T1-weighted sequences were used to detect MVO and IS. An intravenous contrast agent dose of 0.1 mmol/kg gadolinium contrast agent (Gadoterate meglumine, Dotarem, Guerbet S.A., France) was used. The presence of MVO and late gadolinium enhancement (LGE) was assessed by early and late post-contrast imaging acquired respectively 2–5 and 10–20 min following contrast administration. Inversion time was individually adapted to suppress the signal of normal remote myocardium (usual range, 220 to 350 ms). At 4 months follow-up, the same CMR protocol was repeated except for T2-weighted sequences.

Image analysis

The following parameters were measured: left ventricular (LV) end-diastolic volume indexed for body surface area (LVEDVi), left ventricular end-systolic volume indexed (LVESVi), left ventricular ejection fraction (LVEF) and LV mass indexed (LVmass/i). On T2-weighted images, AAR was identified as the myocardial tissue with signal intensity (SI) > 2SD above mean SI of remote myocardium; when present, the internal hypointense core reflecting haemorrhagic component was included. Then, AAR was quantified using a semi-automatic approach, and its extent was expressed as percentage of LV mass. On early post-contrast imaging, MVO was defined as the hypoenhanced region within the hyperintense myocardium. On late post-contrast imaging, LV LGE was automatically identified as the myocardium with SI > 5SD mean SI of remote myocardium.[6] MVO, when present, was included in LGE area. Infarct location was assigned according to the location of the LGE and/or oedema. Infarction was defined as anterior when at least one of the following segments was involved: basal anteroseptal, mid-anterior, mid-anteroseptal or apical anterior segment.[7]

Transmural infarction was defined as >75% hyperenhancement of the LV wall thickness in late post-contrast imaging. STEMI patients were divided in two subgroups according to baseline LVEF using a cut-off of 50% (preserved LVEF and reduced LVEF).

Left ventricular adverse remodelling was defined as a relative increase in LVESV of at least 15% compared with baseline (ΔLVESV $\geq$ 15%).

Cardiac magnetic resonance feature tracking

Left ventricular global longitudinal strain (GLS) and global circumferential strain (GCS) were measured using a CMR feature tracking technique from the same endocardial border traced for HDFs estimation (QStrain Version 1.3.0.79; Medis, Leiden, the Netherlands). Both endocardial (-endo) and transmural (-myo) value were reported in this study.

Left ventricular haemodynamic forces assessment

Left ventricular HDFs were computed from a combination of multiple intersected breath-hold steady-state free-precession cineMR long axis data sets (corresponding to 4, 2 and 3 chamber view), using a dedicated software (QStrain Version 1.3.0.79; Medis, Leiden, the Netherlands). HDFs were estimated using the same endocardial border tracking used for strain calculation. The mathematical model was previously described and validated against 4D flow MRI.[8] The endocardial borders were traced at the end-systolic frame from the three apical views and then tracked frame-by-frame. The 3D LV endocardial surface was reconstructed from the long axis borders. The total HDF vector was evaluated by computing the integral balance of momentum inside LV volume. HDFs curves over time and a polar histogram of HDFs' distribution in the LV were generated (*Figure 1*). As a measure of the overall force amplitude, the dimensionless root mean square of HDFs was computed over the selected period of time: entire cardiac cycle, systole and diastole. In order to compare

Figure 1 From left to right: Cine CMR long axis data sets are used for left ventricular haemodynamic forces estimation. End-systolic and end-diastolic borders are traced and tracked frame-by-frame to allow endocardial border movement reconstruction in a three-dimensional model. Apex-to-base and latero-septal haemodynamic forces are estimated over time and graphically represented as curves. Haemodynamic forces distribution in a selected period of time is represented using a polar plot. 2C, two chamber view; 3C, three chamber view; 3D, three-dimensional; 4C, four chamber view; A, apex; B, base; ED, end-diastole; ES, end-systole; HDFs, haemodynamic forces; L, lateral wall; MR, magnetic resonance; S, septum.
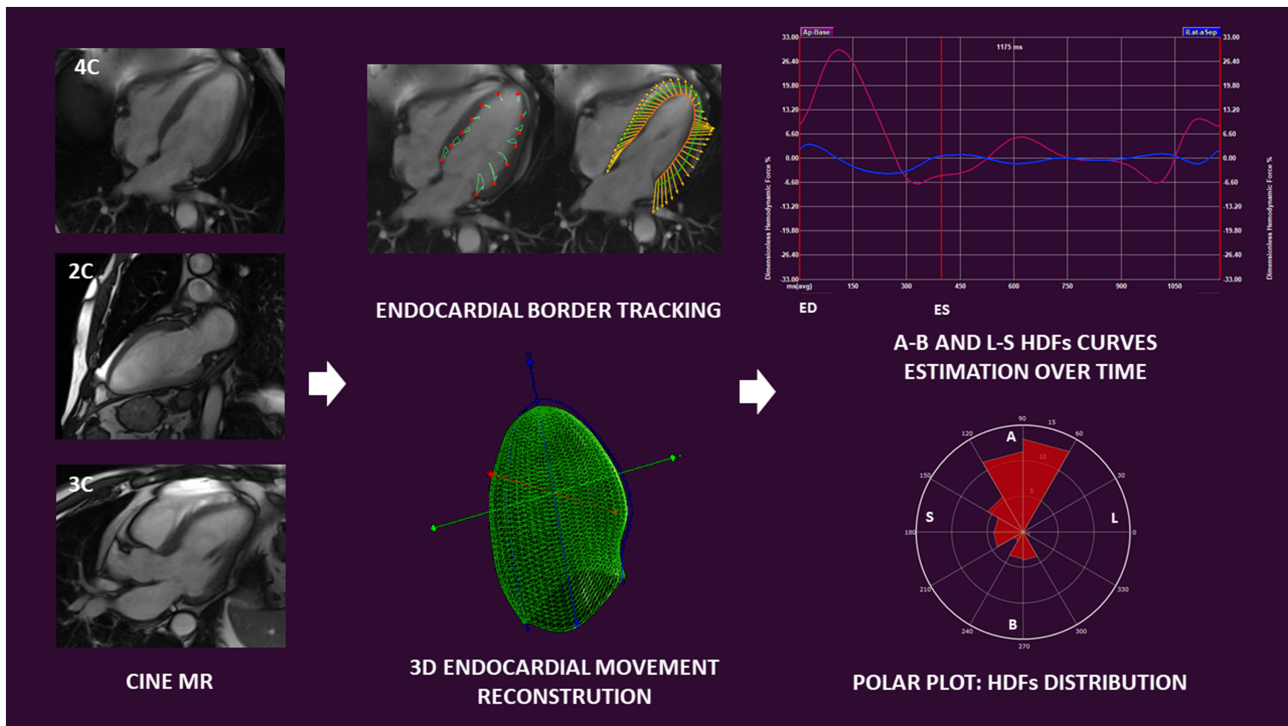
patients with different LV size, the HDFs were normalized with the LV volume and expressed as a percentage of gravity acceleration. These normalized forces represent the average value of pressure gradients in the LV cavity towards different directions, without a direct dependence on the volume size.

The following parameters are calculated in systole, diastole and over the entire cardiac cycle:

- 'apex-to-base' (A-B, longitudinal) HDFs (%): the normalized entity of HDFs directed in the apex-to-base direction;
- 'latero-septal' (L-S, horizontal) HDFs (%): the normalized entity of HDFs directed in the latero-septal direction;
- L-S/A-B HDFs ratio (%): the ratio between L-S HDFs and A-B HDFs was used to assess the relative distribution of the HDF directions in the LV;
- HDFs angle [φ (°)]: the main direction of HDFs over a selected period of time, using a polar coordinate system. φ ranges from 0°, when the HDFs are directed in infero-lateral direction, to 360°, after a circular full turn.

Intra-observer and inter-observer variability

Intra-observer and inter-observer variability for measurements of HDFs were assessed in a sample of 10 patients. Two investigators measured blinded the same exam, and one investigator repeated the analysis 1 week later, blinded to the previous measurements.

Statistical analysis

Continuous variables are presented as mean ± SD and were compared using Student's *t*-test or the Mann–Whitney rank sum test for unpaired and paired comparisons, as appropriate. Comparisons between more than two groups were performed by two-way ANOVA with post-hoc Bonferroni correction. The categorical variables are expressed as counts and percentages and compared by χ^2 test or by Fisher's exact, as appropriate. Spearman correlation coefficient (*r*) was used to test correlation between continuous variables. Univariate logistic analysis was used to determine the

association of demographic, CMR and HDFs variables with adverse LV remodelling at follow-up. Then, all significant univariate risk factors were included in two different multivariate logistic models developed for testing separately collinear variables. Interclass correlation coefficients were calculated to assess inter-observer and intra-observer agreement of HDFs measurements. All tests were two-tailed at 5% significance level, except for multiple comparisons. In that case a Bonferroni-corrected alpha level was applied by dividing the alpha value by the number of comparisons (P value = 0.05/18 = 0.0015). Statistical analyses were performed using the Statistical Package for Social Sciences, Version 23.0 (SPSS, Chicago, IL).

Results

Segment elevation myocardial infarction patients vs. controls

General characteristics and CMR findings of whole STEMI population are depicted in *Tables 1* and *2*, respectively. STEMI patients were divided in two subgroups according to baseline LVEF and then, compared with HC (*Table 3*). STEMI patients with reduced LVEF had lower values of HDFs measured along A-B direction during the entire heartbeat and in systole, as

Table 2 CMR parameter baseline and at 4 months follow-up

Parameters	STEMI Pts, $n = 49$
Baseline	
LVEF (%)	48 ± 10
LVEDVi (mL/m^2)	67 ± 13
ESVi (mL/m^2)	36 ± 12
SVi (mL/m)	33 ± 6
LVmass/i (g/m^2)	62 ± 12
AAR (%)	26 ± 21
IS (%)	18 ± 13
MVO, n (%)	22 (45%)
Transmural MI (%)	19 (39%)
4 months FU	
LVEF (%)	50 ± 10
EDVi (mL/m^2)	74 ± 22
ESVi (mL/m^2)	38 ± 20
SVi (mL/m^2)	36 ± 6
LVmass/i (g/m^2)	58 ± 11
IS (%)	14 ± 12

AAR, area at risk; EDVi, end-diastolic volume index; ESVi, end-systolic volume index; IS, infarct size; LVEDVi, left ventricular end-diastolic volume indexed; LVEF, left ventricular ejection fraction; LVmass/i, left ventricular mass index; MI, myocardial infarction; MVO, microvascular obstruction; SVi, stroke volume index.

compared with HC (A-B HDFs entire heartbeat: 13 ± 6 vs. 22 ± 6; $P = 0.001$), (systolic A-B HDFs: 19 ± 8 vs. 31 ± 9; $P = 0.001$). STEMI patients with preserved LVEF showed intermediate A-B HDFs values both in systole and over the entire heartbeat. L-S HDFs were slightly lower in patients with re-

Table 1 General characteristic of the STEMI population

Parameter	STEMI Pts, $n = 49$	Adverse remodelling, $n = 18$ (37%)	Non-adverse remodelling, $n = 31$ (63%)	P
Age (years)	57 ± 10	59 ± 11	56 ± 10	0.726
Weight (kg)	80 ± 10	79 ± 11	81 ± 9	0.811
Height (cm)	172 ± 6	173 ± 5	172 ± 7	0.593
BMI (kg/m^2)	27 ± 3	26 ± 3	25 ± 2	0.689
cTnI peak (ng/L)	44 ± 75	44 ± 86	44 ± 71	0.754
SBP pre-PCI (mmHg)	124 ± 17	120 ± 19	126 ± 16	0.725
DBP pre-PCI (mmHg)	76 ± 9	72 ± 12	77 ± 7	0.411
HR pre-PCI (bpm)	73 ± 9	71 ± 8	74 ± 9	0.434
Door-to-balloon (min)	184 ± 286	135 ± 174	212 ± 334	0.471
Time-to-PCI (min)	248 ± 837	274 ± 246	247 ± 1,000	0.754
Male sex, n (%)	46 (94%)	17 (94%)	29 (94%)	0.679
Diabetes, n (%)	6 (12%)	5 (28%)	2(6%)	0.08
Hypertension, n (%)	31 (63%)	8 (44%)	24 (77%)	0.047
Family history for CAD, n (%)	27 (55%)	10 (56%)	16 (52%)	0.74
Active smoker, n (%)	25 (51%)	8 (44%)	17 (55%)	0.69
Dyslipidaemia, n (%)	26 (53%)	6 (33%)	17(55%)	0.188
Prodromal angina, n (%)	9 (18%)	6 (33%)	3 (10%)	0.065
Killip class 1, n (%)	42 (86%)	16 (89%)	25 (81%)	0.311
Killip class 2, n (%)	7 (14%)	1 (5%)	6 (19%)	
Anterior STEMI, n (%)	31 (63%)	13 (72%)	18 (58%)	0.305
Non-anterior STEMI, n (%)	18 (37%)	5 (28%)	13 (42%)	
RCA dominant, n (%)	26 (53%)	15 (83%)	29 (94%)	0.362
TIMI flow grade 0/1 pre-PCI, n (%)	48 (98%)	18 (100%)	29 (94%)	0.745
TIMI flow grade 2/3 pre-PCI, n (%)	1 (2%)	0 (0%)	2 (6%)	
TIMI flow grade 0/1 post-PCI, n (%)	0 (0%)	0 (0%)	0 (0%)	0.99
TIMI flow grade 2/3 post-PCI, n (%)	49 (100%)	18 (100%)	31 (100%)	

BMI, body mass index; CAD, coronary artery disease; CKMB, creatine kinase MB; cTnI, cardiac Troponin I; DPB, diastolic blood pressure; HR, heart rate; PCI, percutaneous coronary intervention; RCA, right coronary artery; SBP, systolic blood pressure; STEMI, segment elevation myocardial infarction; TIMI, thrombolysis in myocardial infarction.

Table 3 Feature tracking and haemodynamic forces analysis: STEMI patients and reduced EF vs. STEMI patients and preserved EF vs. healthy controls

	STEMI EF < 50%, n = 21	STEMI EF > 50%, n = 28	Healthy controls, n = 21	P	Post-hoc analysis		
					P^a	P^b	P^c
Feature tracking analysis							
EF (%)	41 ± 5	57 ± 6	63 ± 3	0.001	0.001	0.001	0.020
GLS-endo (%)	−9 ± 2	−17 ± 3	−21.7 ± 2	0.001	0.008	0.001	0.001
GLS-myo (%)	−9 ± 2	−14 ± 8	−21 ± 2	0.001	0.890	0.001	0.003
GCS-endo (%)	−20 ± 3	−28 ± 3	−31 ± 2	0.001	0.001	0.001	0.284
GCS-myo (%)	−13 ± 1	−20 ± 3	−20 ± 1	0.001	0.001	0.001	0.890
GRS (%)	36 ± 12	55 ± 10	65 ± 14	0.001	0.03	0.001	0.076
Haemodynamic forces: entire heart cycle							
A-B (%)	13 ± 6	15 ± 4	22 ± 6	0.001	0.958	0.001	0.002
L-S (%)	2.6 ± 1.3	2.6 ± 0.6	3.6 ± 0.6	0.002	0.980	0.002	0.003
L-S/A-B HDF ratio (%)	20 ± 6	18 ± 4	16 ± 4	0.051	0.244	0.059	0.970
Angle φ (°)	73 ± 3	75 ± 3	74 ± 3	0.016	0.014	0.267	0.469
Haemodynamic forces: systole							
A-B (%)	19 ± 8	23 ± 5	31 ± 9	0.001	0.391	0.001	0.014
L-S (%)	3.3 ± 1.9	3.6 ± 1	4 ± 1	0.046	0.962	0.053	0.268
L-S/A-B HDF ratio (%)	18 ± 6	16 ± 4	15 ± 5	0.229	0.908	0.271	0.987
Impulse angle φ (°)	74 ± 4	76 ± 7	76 ± 4	0.173	0.394	0.267	0.965
Haemodynamic forces: diastole							
A-B (%)	9 ± 7	10 ± 6	13 ± 4	0.038	0.965	0.052	0.176
L-S (%)	2 ± 1.5	1.8 ± 0.7	3 ± 0.9	0.002	0.985	0.010	0.002
L-S/A-B HDF ratio (%)	25 ± 13	20 ± 6	23 ± 7	0.227	0.363	0.985	0.777
Impulse angle φ (°)	72 ± 6	76 ± 4	72 ± 5	0.059	0.111	0.9886	0.096

A-B, apex-base; EF, ejection fraction; GCS-endo, endocardial global circumferential strain; GCS-myo, transmural global circumferential strain; GLS-endo, endocardial global longitudinal strain; GLS-myo, transmural global longitudinal strain; GRS, global radial strain; HDFs, haemodynamic forces; L-S, latero-septal; STEMI, segment elevation myocardial infarction.
[a]STEMI EF < 50% vs. STEMI FE > 50%.
[b]STEMI EF < 50% vs. controls.
[c]STEMI EF > 50% vs. controls.

duced LVEF compared with HC, but without statistical significance. Considering the whole enrolled population, both A-B HDFs and L-S HDFs, calculated over the entire cardiac cycle, showed good linear correlation with LVEF ($r = 0.7$, $P = 0.001$ and $r = 0.6$, $P = 0.001$ respectively), GLS-endo ($r = −0.7$, $P = 0.001$ and $r = −0.6$, $P=0.001$ respectively) and GCS-endo ($r = −0.6$, $P = 0.001$ and $r = −0.5$, $P = 0.001$ respectively). Diastolic L-S/A-B HDF ratio did not differ comparing both STEMI groups with HC.

Location and extension of myocardial infarction

Segment elevation myocardial infarction population was divided according to infarct location in anterior STEMI (63%) and non-anterior STEMI (37%) (Supporting Information, *Tables S1* and *S2*). Anterior STEMI had larger IS (32 ± 21 vs. 14 ± 13; $P = 0.012$) and AAR (22 ± 14 vs. 11 ± 10; $P = 0.016$) at baseline and greater values of IS at 4 months FU. Feature tracking analysis showed that anterior STEMI had lower values of GLS (GLS-endo: −12 ± 4 vs. −18 ± 3; $P = 0.001$ and GLS-myo: −12 ± 4 vs. −13 ± 5; $P = 0.02$) while no significant differences in GCS and GRS were detected. Anterior STEMI had lower values of L-S HDF measured both in systole (2.8 ± 0.9 vs. 3.9 ± 1; $P = 0.01$) and during the entire cardiac

cycle (2.2 ± 0.6 vs. 2.8 ± 0.6; $P = 0.01$). Interestingly, patients with IS over the median (15%) had significantly higher diastolic L-S/A-B HDF ratio (25 ± 10 vs. 20 ± 10; $P = 0.028$) while difference in L-S HDF did not reach statistical significance (2.9 ± 1.5 vs. 3.5 ± 0.7; $P = 0.074$).

Adverse left ventricular remodelling

Clinical characteristics of patients with and without aLVr are reported in *Table 1*. CMR findings comparing patients with and without adverse LV remodelling at 4 months FU are summarized in *Table 4*. We observed greater value of IS (23 ± 16 vs. 15 ± 11; $P = 0.03$) in patients with adverse remodelling, while AAR did not reach statistical significance (32 ± 23 vs. 22 ± 18; $P = 0.07$). In patients with aLVr at FU, baseline systolic L-S HDFs were lower (2.7 ± 0.9 vs. 3.6 ± 1; $P = 0.027$) while diastolic L-S/A-B HDF ratio was significantly higher (28 ± 14 vs. 19 ± 6; $P = 0.03$) (*Table 5*) (*Figure 2*). Accordingly, impulse diastolic HDF angle was lower in patients with adverse remodelling (71 ± 7 vs. 75 ± 4; $P = 0.03$).

At univariate logistic regression analysis, higher IS [odds ratio (OR) 1.05; 95% confidence interval (95% CI) 1.0–11.1; $P = 0.04$], lower L-S HDFs (OR 0.41; 95% CI 0.2–0.9;

Table 4 CMR findings comparing patient with vs. without adverse remodelling

	STEMI, n = 49		
	Adverse remodelling, n = 18 (37%)	Non-adverse remodelling, n = 31 (63%)	P
Baseline			
EF (%)	48 ± 11	47 ± 9	0.868
EDVi (mL/m^2)	68 ± 13	70 ± 13	0.427
ESVi (mL/m^2)	35 ± 13	37 ± 13	0.471
SV/i (mL/m^2)	32 ± 6	33 ± 6	0.726
LVmass/i (g/m^2)	59 ± 11	64 ± 13	0.289
AAR (%)	32 ± 23	22 ± 18	0.070
IS (%)	23 ± 16	15 ± 11	0.030
MVO, n (%)	7 (39%)	17 (54%)	0.462
Transmurality, n (%)	10 (56%)	9 (29%)	0.09
4 months FU			
LVEF (%)	45 ± 11	53 ± 8	0.060
EDV/i (mL/m^2)	87 ± 27	66 ± 15	0.053
ESV/i (mL/m^2)	50 ± 25	31 ± 12	0.005
SV/i (mL/m^2)	37 ± 7	36 ± 6	0.726
LVmass/i (g/m^2)	54 ± 11	60 ± 11	0.326
IS (%)	16 ± 14	12 ± 10	0.580

AAR, area at risk; EDVi, end-diastolic volume index; ESVi, end-systolic volume index; IS, infarct size; LVEF, left ventricular ejection fraction; LVmass/i, left ventricular mass index; MVO, microvascular obstruction; SVi, stroke volume index; STEMI, segment elevation myocardial infarction.

Table 5 Feature tracking and haemodynamic forces analysis comparing patient with vs. without adverse remodelling

	STEMI, n = 49		
	Adverse remodelling, n = 18 (37%)	Non-adverse remodelling, n = 31 (63%)	P
Feature tracking analysis			
GLS-endo (%)	−13 ± 5	−15 ± 5	0.308
GLS-myo (%)	−13 ± 5	−12 ± 8	0.782
GCS-endo (%)	−25 ± 5	−25 ± 6	0.782
GCS-myo (%)	−17 ± 4	−18 ± 4	0.494
GRS (%)	46 ± 15	49 ± 15	0.811
Haemodynamic forces: entire heart cycle			
A-B (%)	12 ± 4	14 ± 5	0.308
L-S (%)	2.2 ± 0.5	2.6 ± 0.7	0.212
L-S/A-B HDFs ratio (%)	19 ± 6	19 ± 4	0.645
Angle φ (°)	74 ± 3	74 ± 2	0.726
Haemodynamic forces entire: systole			
A-B (%)	18 ± 5	21 ± 6	0.213
L-S (%)	2.7 ± 0.9	3.6 ± 1	0.027
L-S/A-B HDFs ratio (%)	15 ± 4	18 ± 5	0.141
Impulse angle φ (°)	76 ± 3	75 ± 3	0.291
Haemodynamic forces entire: diastole			
A-B (%)	8 ± 7	9 ± 7	0.567
L-S (%)	1.9 ± 0.8	1.7 ± 1	0.187
L-S/A-B HDFs ratio (%)	28 ± 14	19 ± 6	0.030
Impulse angle φ (°)	71 ± 7	75 ± 4	0.03

A-B, apex-base; GCS-endo, endocardial global circumferential strain; GCS-myo, transmural global circumferential strain; GLS-endo, endocardial global longitudinal strain; GLS-myo, transmural global longitudinal strain; GRS, global radial strain; HDFs, haemodynamic forces; L-S, latero-septal; STEMI, segment elevation myocardial infarction.

P = 0.04), lower diastolic HDFs angle (OR 0.8; 95% CI 0.7–0.99; P = 0.03) and higher diastolic L-S/A-B HDFs ratio (OR 1.1; 95% CI 1.01–1.2; P = 0.05) were associated with aLVr at FU. In order to avoid collinearity, L-S/A-B HDFs ratio and diastolic HDFs angle were tested separately at multivariate logistic regression. In the multivariable logistic regression analysis, L-S/A-B HDF ratio and diastolic HDF angle remained the only independent predictors of adverse LV remodelling after correction for other baseline determinants (*Table 6*). Considering LV remodelling as a continuous variable, systolic L-S HDFs showed negative linear correlation with the relative variation in end-systolic volume [ΔLV-ESV(%)] (r = −0.5, P = 0.001) and end-diastolic volume [ΔLV-EDV(%)] (r = −0.5, P = 0.001) at 4 months FU, while correlated positively with LVEF at 4 months FU (r = 0.4, P = 0.001). At the same time, diastolic L-S/A-B HDF ratio correlated positively with ΔLV-ESV(%) (r = 0.4, P = 0.001), ΔLV-EDV(%) (r = 0.4, P = 0.001) and negatively with LVEF at 4 months (r = −0.5, P = 0.001).

Intra-observer and inter-observer agreement

Both intra-observer and inter-observer agreement were good to excellent for all HDFs parameters. Interclass correlation co-efficients are reported in *Table S3*.

Discussion

In the present paper, the behaviour of HDFs, in a cohort of STEMI patients, is described for the first time. Our results showed that (1) STEMI patients had lower values of HDFs measured along A-B direction as compared to healthy individuals, (2) patients with anterior STEMI had lower values of L-S HDFs both in systole and during the entire cardiac cycle compared with non-anterior MI, (3) patients with larger MI had higher diastolic L-S/A-B HDFs ratio and (4) patients with aLVr at FU had lower baseline systolic L-S HDFs and higher diastolic L-S/A-B HDFs ratio.

Adverse remodelling following acute myocardial infarction

The present paper suggests a critical role of HDFs in cardiac adaptations following acute MI and seems to confirm the hypothesis that intraventricular forces distribution is involved in mechanisms inducing LV remodelling.

Post-infarct adverse LV remodelling is a complex phenomenon involving both infarcted and remote myocardium. The pathophysiology of remodelling includes infarct expansion, chamber dilatation and ventricular hypertrophy as a consequence of increased preload and afterload.[9] Neurohormonal

Figure 2 Polar plots representing diastolic haemodynamic forces distribution in two different patients. On the left: a patient without adverse remodelling at follow-up; at baseline diastolic haemodynamic forces distribution were normally oriented with low diastolic latero-septal over apex-base ratio. On the right: a patient with adverse remodelling at follow-up; at baseline, misaligned diastolic haemodynamic forces with high diastolic latero-septal over apex-base ratio. A, apex; B, base; HDFs, haemodynamic forces; L, lateral wall; S, septum.
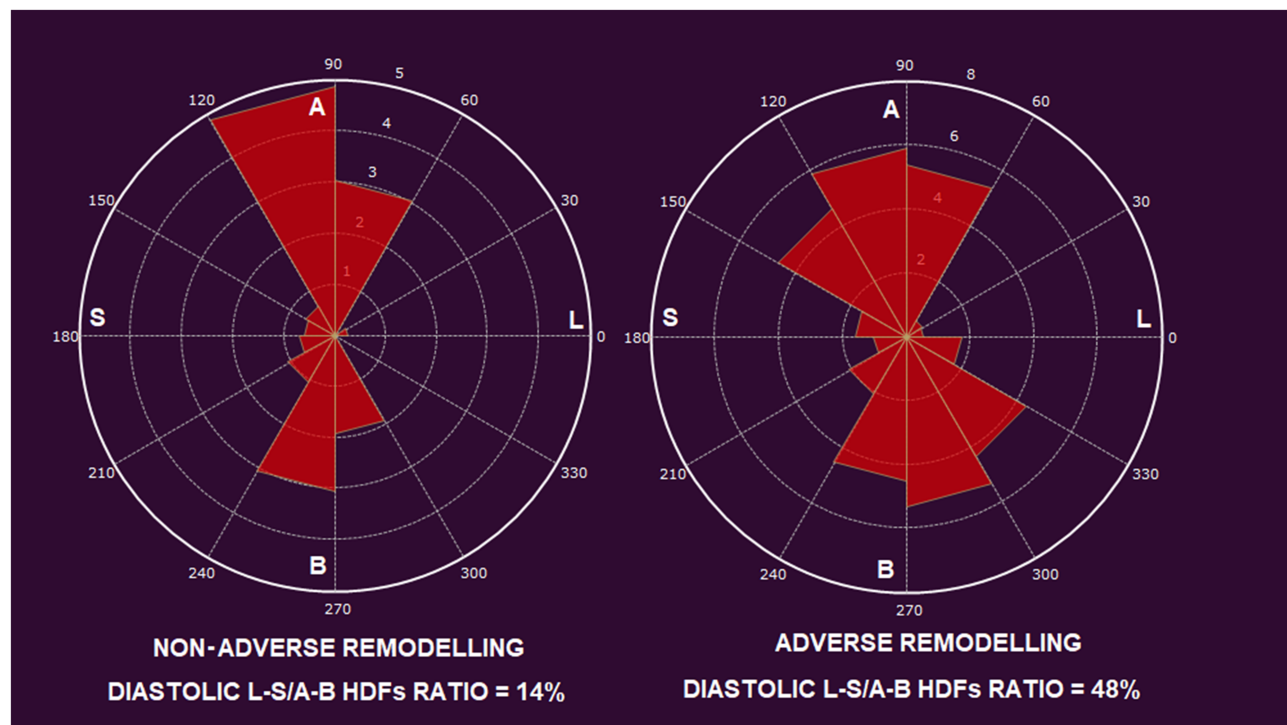

Table 6 Univariate and multivariate logistic regression for adverse remodelling

Parameter	Univariate		Multivariate (Model 1)		Multivariate (Model 2)	
	OR (95% CI)	*P*	OR (95% CI)	*P*	OR (95% CI)	*P*
IS (%)	1.05 (1.01–1.1)	0.04	—	—	—	
Systolic L-S HDF (%)	0.41 (0.2–0.9)	0.04	—	—	—	
Diastolic L-S/A-B HDF ratio (%)	1.1 (1.01–1.2)	0.05	1.1 (1.01–1.2)	0.04	n.a.	
Diastolic impulse angle φ (°)	0.8 (0.7–0.99)	0.03	n.a.		0.88 (0.8–0.99)	0.03

A-B, apex-base; HDFs, haemodynamic forces; L-S: latero-septal.

responses, oxidative stress, cytokine activation and cellular hypertrophy are widely implicated in scar formation and in ultrastructural changes in remote myocardium.[10] After myocardial infarction, misbalance in forces generated by non-symmetrical LV contraction has been integrated in this pathogenic model, connecting remodelling occurring both in infarct and remote myocardium.[11] Moreover, LV systolic mechanical dyssynchrony has been proposed as a predictor of post-infarct aLVr.[12] However, intraventricular forces distribution was only assumed on basis of LV wall motion mechanics but neither measured nor calculated. Analysis of intraventricular flow energetic properties in STEMI patients, using Echo-PIV technique, showed different values of energy dissipation in patients with distinct grade of LV systolic dysfunction.[13]

Weaker haemodynamic forces after segment elevation myocardial infarction

Lower values of HFDs after STEMI are likely to be related to the loss of viable myocardium participating in cardiac contraction, with consequent reduction of blood acceleration towards LV outflow tract. The significant linear correlation between HDFs (A-B and L-S) and LVEF further supports this hypothesis. While A-B forces reflect systolic overall function, systolic L-S HDFs reflect early blood acceleration from the inlet to the outflow tract due to the so-called 'direct flow'.[14] In patients with systolic dysfunction, direct flow is reduced while the 'retained flow' increases.[15] In our study, lower values of L-S systolic HDFs were found in anterior STEMI as compared with non-anterior ones.

Systolic haemodynamic forces and adverse remodelling

In patients with aLVr at FU, baseline systolic L-S HDFs were lower, reflecting lower forces generated by accelerating blood flow proceeding out the LV outflow tract. According to previous reports, healthy patients have non-negligible HDFs directed in L-S direction.[14] The presence of systolic L-S intraventricular pressure gradients (IVPGs) in healthy individuals, reflecting the systolic direct flow, has been demonstrated by 4D flow MRI.[14] Less efficient direct redirection of the flow from the inlet to the outflow is associated with aLVr in our study.

Diastolic misalignment of haemodynamic forces and adverse remodelling

In our study, diastolic L-S/A-B HDFs ratio was significantly higher in patients with aLVr. Accordingly, in those patients, impulse diastolic HDFs angle was found slightly deflected towards transversal direction. Both L-S/A-B HDFs ratio and impulse diastolic HDFs angle were independent predictors of post-infarction LV remodelling at 4 months follow-up. While systolic L-S HDFs are the consequence of the direct flow, diastolic L-S HDFs reflect asynergy and asynchrony in LV wall motion.[16] On the other hand, diastolic A-B HDFs are determined by global elastic recoil causing active suction of blood from the base to the apex. Increased L-S/A-B HDFs ratio is the consequence of disproportionately high diastolic L-S HDFs causing significant deflection of the normal flow force momentum or, equivalently, IVPGs. Deflected IVPGs were found in patients with dilated cardiomyopathy when compared with healthy individuals.[17] While HDFs in normal LVs are mainly directed along the base-apex direction, greater diastolic orthogonal forces, reflected by higher L-S/A-B HDFs ratios, characterize dysfunctional and remodelled LVs.[5] These findings are in line with previous reports describing regional inhomogeneity in the development of IVPGs and increased diastolic convective deceleration in dilated cardiomyopathy.[18] Less efficient pumping mechanics, more spherical shape and different LV filling characteristics may contribute to abnormal diastolic flow in this group of patients.[19–21] Moreover, Eriksson et al. found higher L-S/A-B HDFs ratio during the early diastolic filling phase in heart failure patients with left bundle branch block when compared with a matched, non-left bundle branch block, control group.[16] Using Echo-PIV, Pedrizzetti et al. demonstrated that cardiac resynchronization therapy responders had LV forces aligned mainly along the physiological base-apex direction over the entire heartbeat, while flow force direction became more transversal when the pacemaker was temporarily turned off.[22,23] Moreover, reverse LVr (ΔLV-ESV) correlated with the entity of realignment of the HDFs following cardiac resynchronization therapy implantation.[22] Those findings were later confirmed estimating HDFs using a speckle-tracking based technique.[24] Changes in diastolic mechanoreceptors stimulation in endothelial cells may contribute to activation of intracellular pathways involved in cardiac adaptation and remodelling.[25] Deeper comprehension about haemodynamic mechanism involved in LVr after STEMI may help physicians in predicting patients' prognosis and targeting individualized treatment.

Limitation

The most important limit of our study is the small population observed. Therefore, results should be considered as a preliminary observation and must be verified in larger cohorts. No significant clinical outcomes were evaluated due to the limited number of major cardiac event reported during follow-up. While longitudinal HDFs calculation from endocardial border movement is nicely robust, assumptions about intraventricular flow are necessary for transversal forces estimations: intraventricular vortex instabilities are ignored, and mitral inflow and LV outflow jets are assumed to be aligned with LV main axis. However, the use of routine cineMR acquisitions, instead time-consuming 4D flow analysis, may allow non-invasive estimation of IVPGs in routine clinical practice.

Conclusions

Estimation of HDFs from endocardial border movement detected by feature tracking analysis is feasible and may allow IVPGs evaluation in routine clinical scenarios. Patients with aLVr at 4 months FU showed significant misalignment of diastolic HDFs during the early phase of MI. This study suggests the role of HDFs in cardiac adaptations following acute myocardial infarction. Our results should be confirmed in larger prospective studies.

Conflict of interest

All authors have no conflicts of interest to disclose.

Funding

Supporting information

Additional supporting information may be found online in the Supporting Information section at the end of the article.

Table S1. CMR findings comparing patients with anterior and non-anterior STEMI.

Table S2/ Feature tracking and hemodynamic forces analysis: anterior STEMI vs non-anterior STEMI.
Table S3. Intra- and inter-observer agreement for hemodynamic forces measurements.

References

1. Masci PG, Ganame J, Francone M, Desmet W, Lorenzoni V, Iacucci I, Barison A, Carbone I, Lombardi M, Agati L, Janssens S, Bogaert J. Relationship between location and size of myocardial infarction and their reciprocal influences on post-infarction left ventricular remodelling. *Eur Heart J* 2011; **32**: 1640–1648.

2. Galea N, Dacquino GM, Ammendola RM, Coco S, Agati L, De Luca L, Carbone I, Fedele F, Catalano C, Francone M. Microvascular obstruction extent predicts major adverse cardiovascular events in patients with acute myocardial infarction and preserved ejection fraction. *Eur Radiol* 2019; **29**: 2369–2377.

3. Mather AN, Fairbairn TA, Ball SG, Greenwood JP, Plein S. Reperfusion haemorrhage as determined by cardiovascular MRI is a predictor of adverse left ventricular remodelling and markers of late arrhythmic risk. *Heart* 2011; **97**: 453–459.

4. Ponikowski P, Voors AA, Anker SD, Bueno H, Cleland JGF, Coats AJS, Falk V, González-Juanatey JR, Harjola VP, Jankowska EA, Jessup M, Linde C, Nihoyannopoulos P, Parissis JT, Pieske B, Riley JP, Rosano GMC, Ruilope LM, Ruschitzka F, Rutten FH, van der Meer P, Authors/Task Force Members, Document Reviewers. 2016 ESC Guidelines for the diagnosis and treatment of acute and chronic heart failure: the task force for the diagnosis and treatment of acute and chronic heart failure of the European Society of Cardiology (ESC). Developed with the special contribution of the Heart Failure Association (HFA) of the ESC. *Eur J Heart Fail* 2016; **18**: 891–975.

5. Pedrizzetti G, La Canna G, Alfieri O, Tonti G. The vortex—an early predictor of cardiovascular outcome? *Nat Rev Cardiol* 2014; **11**: 545–553.

6. Bondarenko O, Beek AM, Hofman MBM, Kühl HP, Twisk JWR, Van Dockum WG, Visser CA, Van Rossum AC. Standardizing the definition of hyperenhancement in the quantitative assessment of infarct size and myocardial viability using delayed contrast-enhanced CMR. *J Cardiovasc Magn Reson* 2005; **7**: 481–485.

7. Ortiz-Pérez JT, Rodríguez J, Meyers SN, Lee DC, Davidson C, Wu E. Correspondence between the 17-segment model and coronary arterial anatomy using contrast-enhanced cardiac magnetic resonance imaging. *JACC Cardiovasc Imaging* 2008; **1**: 282–293.

8. Pedrizzetti G, Arvidsson PM, Töger J, Borgquist R, Domenichini F, Arheden H, Heiberg E. On estimating intraventricular hemodynamic forces from endocardial dynamics: a comparative study with 4D flow MRI. *J Biomech* 2017; **60**: 203–210.

9. Opie LH, Commerford PJ, Gersh BJ, Pfeffer MA. Controversies in ventricular remodelling. *Lancet* 2006; **367**: 356–367.

10. St. John Sutton MG, Sharpe N. Left ventricular remodeling after myocardial infarction: pathophysiology and therapy. *Circulation* 2000; **101**: 2981–2988.

11. Zhong L, Su Y, Yeo SY, Tan RS, Ghista DN, Kassab G. Left ventricular regional wall curvedness and wall stress in patients with ischemic dilated cardiomyopathy. *Am J Physiol Heart Circ Physiol* 2009; **296**: H573–H584.

12. Zhang Y, Yip GW, Chan AKY, Wang M, Lam WWM, Fung JWH, Chan JYS, Sanderson JE, Yu CM. Left ventricular systolic dyssynchrony is a predictor of cardiac remodeling after myocardial infarction. *Am Heart J* 2008; **156**: 1124–1132.

13. Agati L, Cimino S, Tonti G, Cicogna F, Petronilli V, De Luca L, Iacoboni C, Pedrizzetti G. Quantitative analysis of intraventricular blood flow dynamics by echocardiographic particle image velocimetry in patients with acute myocardial infarction at different stages of left ventricular dysfunction. *Eur Heart J Cardiovasc Imaging* 2014; **15**: 1203–1212.

14. Arvidsson PM, Töger J, Carlsson M, Steding-Ehrenborg K, Pedrizzetti G, Heiberg E, Arheden H. Left and right ventricular hemodynamic forces in healthy volunteers and elite athletes assessed with 4D flow magnetic resonance imaging. *Am J Physiol Circ Physiol* 2017; **312**: H314–H328.

15. Stoll VM, Hess AT, Rodgers CT, Bissell MM, Dyverfeldt P, Ebbers T, Myerson SG, Carlhäll CJ, Neubauer S. Left ventricular flow analysis novel imaging biomarkers and predictors of exercise capacity in heart failure. *Circ Cardiovasc Imaging* 2019; **12**: 8130.

16. Eriksson J, Zajac J, Alehagen U, Bolger AF, Ebbers T, Carlhäll CJ. Left ventricular hemodynamic forces as a marker of mechanical dyssynchrony in heart failure patients with left bundle branch block. *Sci Rep* 2017; **7**: 1–9.

17. Eriksson J, Bolger AF, Ebbers T, Carlhall CJ. Left ventricular hemodynamic forces are altered in patients with dilated cardiomyopathy. *J Cardiovasc Magn Reson* 2015; **17**: 1–2.

18. Yotti R, Bermejo J, Antoranz JC, Desco MM, Cortina C, Rojo-Álvarez JL, Allué C, Martín L, Moreno M, Serrano JA, Muñoz R. A noninvasive method for assessing impaired diastolic suction in patients with dilated cardiomyopathy. *Circulation* 2005; **112**: 2921–2929.

19. Hill JA, Olson EN. Cardiac plasticity. *N Engl J Med*. Massachussetts Medical Society 2008; **358**: 1370.

20. Carlhäll CJ, Bolger A. Passing strange: flow in the failing ventricle. *Circ Heart Fail* 2010; **3**: 326–331.

21. Filomena D, Cimino S, Maestrini V, Cantisani D, Petronilli V, Mancone M, Tonti G, Pedrizzetti G, Agati L. Changes in intraventricular flow patterns after MitraClip implant in patients with functional severe mitral regurgitation. *J Am Soc Echocardiogr*. Mosby Inc. 2019; **32**: 1250–1253.e1.

22. Pedrizzetti G, Martiniello AR, Bianchi V, D'Onofrio A, Caso P, Tonti G. Changes in electrical activation modify the orientation of left ventricular flow momentum: novel observations using echocardiographic particle image velocimetry. *Eur Heart J Cardiovasc Imaging* 2016; **17**: 203–209.

23. Cimino S, Palombizio D, Cicogna F, Cantisani D, Reali M, Filomena D, Petronilli V, Iacoboni C, Agati L. Significant increase of flow kinetic energy in "nonresponders" patients to cardiac resynchronization therapy. *Echocardiography* 2017; **34**: 709–715.

24. Dal Ferro M, De Paris V, Collia D, Stolfo D, Caiffa T, Barbati G, Korcova R, Pinamonti B, Zovatto L, Zecchin M,

Sinagra G, Pedrizzetti G. Left ventricular response to cardiac resynchronization therapy: insights from hemodynamic forces computed by speckle tracking. *Front Cardiovasc Med* 2019; **14**: 6.

25. Pasipoularides A. Diastolic filling vortex forces and cardiac adaptations: probing the epigenetic nexus. *Hellenic J Cardiol* 2012; **53**: 458–469.